

FUNCTIONAL-LEVEL UNCERTAINTY QUANTIFICATION FOR CALIBRATED FINE-TUNING ON LLMs

Ruijia Niu^{1 2}Dongxia Wu^{1 2}Rose Yu^{1 2}Yi-An Ma^{2 1}

ABSTRACT

Accurate uncertainty quantification in large language models (LLMs) is essential for providing credible confidence estimates over their outputs. However, fine-tuned LLMs often exhibit overconfidence in uncertain predictions, which stems from their limited ability to generalize with sparse data. Existing parameter efficient fine-tuning (PEFT) uncertainty quantification methods for LLMs focus on post fine-tuning stage, and thus fail to address the core issue: limited specialization of PEFT adapters to accurately capture task-specific input-output relationships. To address these limitations, we propose Functional-Level Uncertainty Quantification for Calibrated Fine-Tuning (UQ4CT), which captures and calibrates uncertainty over the space of functions that map input prompts to outputs. We implement UQ4CT during the fine-tuning stage via a mixture-of-experts framework that hierarchically decomposes the functional space. Empirically, UQ4CT achieves over 25% reduction in Expected Calibration Error (ECE) while preserving high accuracy across five benchmarks. Even under distribution shift, UQ4CT maintains superior ECE performance with high accuracy, showcasing improved generalizability.

1 Introduction

Quantifying the credibility of outputs has been one of the most important problems around large language models (LLMs) [Chang et al., 2024]. In particular, fine-tuned LLMs often struggle with overconfidence in their outputs due to limited training data, failing to reflect the true credibility of their answers [Xiao et al., 2022, He et al., 2023, Tian et al., 2023, OpenAI, 2023]. Such overconfidence can assert misinformation with high certainty, making it difficult for users to discern truth from falsehood. This has become a crucial problem in safety-critical decision making and scientific domains where data is relatively limited, such as formal proof generation, climate science, and healthcare [Singhal et al., 2022, Wu et al., 2023a, Lampinen et al., 2023, Li et al., 2022]. Methods that enhance uncertainty quantification for fine-tuned LLMs are therefore essential to ensure trustworthy predictions.

One salient challenge of uncertainty quantification in large language models is the trade-off among accuracy, calibration, and efficiency. Ideally, one seeks to calibrate model uncertainty without degrading accuracy or slowing output generation. Recent approaches often focus on prompt perturbation—modifying the model input and quantifying the resulting prediction variance [Hou et al., 2023, Gao et al., 2024]—or sampling multiple completions to measure prediction disagreement [Farquhar et al., 2024]. However, these methods generally assume the model is already well-aligned with the data distribution, and thus struggle to capture uncertainty arising during fine-tuning, especially the generalization gap due to adaptation on limited data. Additionally, since these methods require multiple forward passes per input, they incur significant computational overhead, limiting scalability.

Beyond prompt-level approaches, Bayesian methods and ensemble-based uncertainty quantification have been established for fine-tuned LLMs, often in conjunction with low-rank adaptation (LoRA) [Hu et al., 2021a]. Methods such as Monte Carlo dropout [Gal and Ghahramani, 2016], checkpoint ensembles [Chen et al., 2017], deep ensembles [Lakshminarayanan et al., 2017, Wang et al., 2023, Zhai et al., 2023], and Laplace-LoRA [Yang et al., 2024a] apply Bayesian inference or ensembling over LoRA parameters to capture uncertainty arising from model adaptation and limited data. While Bayesian and ensemble methods estimate uncertainty after fine-tuning by analyzing the learned

¹Department of Computer Science and Engineering, University of California San Diego, La Jolla, California, USA

²Halcioğlu Data Science Institute, University of California San Diego, La Jolla, California, USA
Preprint. Correspondence to: Yian Ma <yianma@ucsd.edu>.

parameter space, they do not address the limitations caused by sparse data during fine-tuning. This post hoc perspective can miss uncertainty that arises when adapting to new tasks with limited data.

To overcome this, we shift focus from parameter-space to functional-space uncertainty quantification. The functional space encompasses the input-output mappings the model can realize, capturing the true variability in its predictions. By calibrating uncertainty at this level during fine-tuning, we ensure the model’s confidence better reflects its actual predictive reliability.

We therefore introduce Functional-Level Uncertainty Quantification for Calibrated Fine-Tuning (UQ4CT), a method that explicitly calibrates functional-level uncertainty in LLMs during fine-tuning. UQ4CT leverages ensembles of LoRA modules at each layer to construct a rich set of basis functions. We then employ a Mixture-of-Experts (MoE) architecture [Li et al., 2024] to hierarchically combine these basis functions, forming a flexible functional space (see Figure 1). During fine-tuning, UQ4CT jointly learns the LoRA expert parameters and calibrates the prompt-dependent function mixture to align functional-level uncertainty with predictive correctness, enabling the model to output calibrated distributions over the functional space.

During inference, LoRA experts offer diverse functional relationships acquired during fine-tuning, while MoE routers dynamically select the most relevant experts for each input prompt. This selection is guided by functional-level uncertainty calibration performed throughout fine-tuning, which aims to optimize the choice of the correct functional relationship for each prompt. More accurate expert selection enables the model to learn diverse functional relationships. As a result, the model’s uncertainty estimates become better aligned, enhancing calibration without compromising accuracy. To summarize, our contributions include:

- A novel uncertainty quantification approach for LLMs with MoE architecture during fine-tuning to quantify functional-level uncertainty and align with the probability of predictive correctness, which mitigates overconfidence issue and improves generalizability.
- A new calibration loss that incorporates predictive correctness probability to dynamically align the prompt-dependent LoRA mixture for better uncertainty estimation.
- Hierarchical decomposition of functional-level uncertainty into layer-wise mixture weights with guarantee that our calibration loss aligns mixture weights with predictive correctness.
- More than 25% expected calibration error (ECE) reduction on 4 common-sense reasoning tasks and 1 domain-specific question answering task; improved ECE performance without compromising accuracy *under distribution shift* on 2 common-sense reasoning tasks and 4 domain-specific question answering tasks.

2 Preliminaries

Low-rank Adaptation (LoRA). LLMs have numerous large weight matrices to perform matrix multiplication, denoted as $\mathbf{W}_0 \in \mathbb{R}^{n_{\text{out}} \times n_{\text{in}}}$ that maps inputs \mathbf{x} to outputs \mathbf{h} . Hu et al. [2021a] proposes LoRA, which fixes \mathbf{W}_0 and introduces a low-rank perturbation $\Delta\mathbf{W}$ to the weight matrix:

$$\mathbf{h} = \mathbf{W}_0\mathbf{x} + \Delta\mathbf{W}\mathbf{x} = \mathbf{W}_0\mathbf{x} + \mathbf{B}\mathbf{A}\mathbf{x}. \quad (1)$$

Here, $\Delta\mathbf{W}$ is calculated as the product of two matrices, $\mathbf{B} \in \mathbb{R}^{n_{\text{out}} \times n_{\text{lr}}}$ and $\mathbf{A} \in \mathbb{R}^{n_{\text{lr}} \times n_{\text{in}}}$ where n_{lr} is significantly smaller than n_{in} or n_{out} . For example, we use $n_{\text{lr}} = 32$ while $n_{\text{in}} = n_{\text{out}} = 4096$ for the Llama2-7b model [Touvron

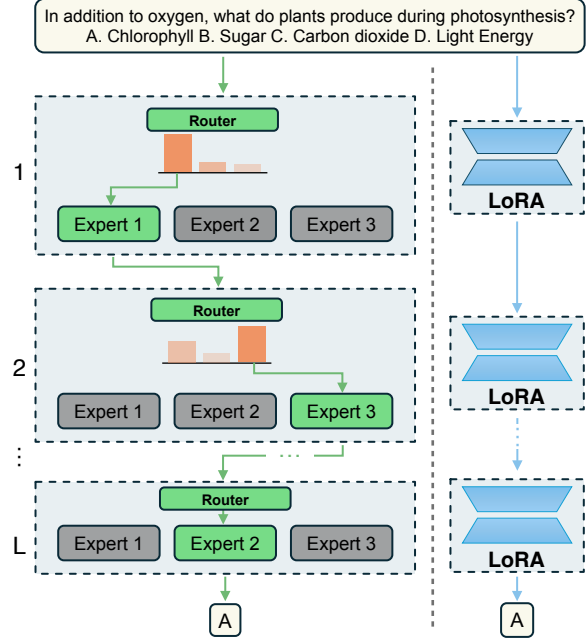


Figure 1: Left: The Mixture of Experts (MoE) architecture captures diverse functional relationships by dynamically routing inputs to different expert modules based on the prompt. Right: The standard LoRA approach lacks such functional-space diversity, limiting its capacity to capture variations in the functional relationships during fine-tuning.

et al., 2023a]. Therefore, the total number of LoRA parameters for this $\Delta \mathbf{W}$ is $n_{\text{lr}}(n_{\text{in}} + n_{\text{out}})$, which is far smaller than the parameter count of the full matrix, $n_{\text{in}}n_{\text{out}}$. One of the key motivations of incorporating LoRA to fine-tune LLMs is the vast amount of memory cost reduction compared with fine-tuning on the full model. For an LLM with 7 billion parameters, maintaining the average gradient and average squared gradients for optimization multiplies the memory required by a factor of 3 compared to simply loading model weights. LoRA greatly mitigates this memory cost as the tripled memory consumption only applies to LoRA adapters.

Mixture of Experts (MoE). LoRA Mixture-of-Experts [Li et al., 2024, Wu et al., 2024a] is an efficient approach to scale the number of parameters while maintaining the same computational bounds. LoRA MoE utilizes the top-k router to assign each token to the LoRA experts [Lepikhin et al., 2020]. The router is a linear layer that maps the input hidden state \mathbf{h} to a probability distribution of candidate experts.

The plain transformer block in a large language model consists of the q, k, v encoding layers ($\text{FFN}_{q,k,v}$), layer norm (LN) and the feedforward layer (FFN), together with residual connections. Formally, given \mathbf{h}^1 as the tokenized input text, the output of ℓ -th layer is generated as:

$$\mathbf{z}^\ell = f_{\text{attn}}(\text{FFN}_{q,k,v}(\text{LN}(\mathbf{h}^{\ell-1}))) + \mathbf{h}^{\ell-1}, \quad \mathbf{h}^\ell = \text{FFN}(\text{LN}(\mathbf{z}^\ell)) + \mathbf{z}^\ell. \quad (2)$$

Here, f_{attn} represents the attention calculation step.

Let $\mathbf{h}^\ell \in \mathbb{R}^{1 \times d}$ ($1 \leq \ell \leq L$) denote the output hidden state at the ℓ -th layer of the LLM, where L is the number of LLM layers and d is the hidden dimension. With \mathbf{W}_r^ℓ as the trainable router weight at layer ℓ , the top-k gate router $\tilde{R}(\cdot)$ chooses k experts with highest probability given a hidden state \mathbf{h}^ℓ :

$$\tilde{R}^\ell(\mathbf{h}^\ell) = \text{Keep-Top-}k(\text{Softmax}(\mathbf{W}_r^\ell \cdot \mathbf{h}^\ell)). \quad (3)$$

Finally, we obtain the final MixLoRA prediction with:

$$\text{MixLoRA}(\mathbf{h}^\ell) = \sum_{k=1}^K \tilde{R}^\ell(\mathbf{h}^\ell)_k E_k^\ell(\mathbf{h}^\ell), \quad E_k^\ell(\mathbf{h}^\ell) = \mathbf{W}_{pre}^\ell \cdot \mathbf{h}^\ell + \mathbf{B}_k^\ell \mathbf{A}_k^\ell \cdot \mathbf{h}^\ell \quad (4)$$

where \mathbf{W}_{pre}^ℓ is the frozen pretrained weight at layer ℓ and $\mathbf{B}_k^\ell \mathbf{A}_k^\ell$ is the k -th LoRA expert.

With MixLoRA defined in Equation 4, we can apply MixLoRA layers at q, k, v encoding and FFN layers:

$$\mathbf{z}^\ell = f_{\text{attn}}(\text{MixLoRA}_{q,k,v}(\text{LN}(\mathbf{h}^{\ell-1}))) + \mathbf{h}^{\ell-1}, \quad \mathbf{h}^\ell = \text{MixLoRA}(\text{LN}(\mathbf{z}^\ell)) + \mathbf{z}^\ell. \quad (5)$$

3 Methodology

The high-level goal of UQ4CT is to leverage the ensemble of prompt-dependent LoRA mixture-of-experts (MoE) to guide and calibrate the confidence of the model during fine-tuning. By quantifying the variability in how different LoRA experts are combined for each input, UQ4CT enables the model to adaptively select expert mixtures that reflect the true uncertainty in its predictions. Our approach not only encourages the model to exploit confident expert combinations for accurate predictions but also promotes exploration of alternative experts when uncertainty is high, ultimately leading to better-calibrated and more reliable model outputs.

3.1 Decomposition of the Functional Space

Given the immense size of both the pre-training dataset and the model, we posit that the pretrained network contains submodules capable of expressing a wide range of functional relationships present in the data. During fine-tuning, our focus is on the functional space spanned by the model, which can be effectively captured as a mixture of LoRA experts, each representing a distinct basis function. However, naively decomposing the full functional space by considering all possible combinations of these experts quickly leads to a combinatorial explosion.

Naive Decomposition. Denote the input prompt as \mathbf{x} and the functional map from input to output as f . A straightforward approach is to express the function as a sum over all possible compositions of K submodules per layer, across L layers:

$$f(\mathbf{x}) = \sum_{k^1, \dots, k^L=1}^K \alpha_{k^1, \dots, k^L} g_{k^L}^L \left(\dots \left(g_{k^1}^1 (\mathbf{x}) \right) \right), \quad (6)$$

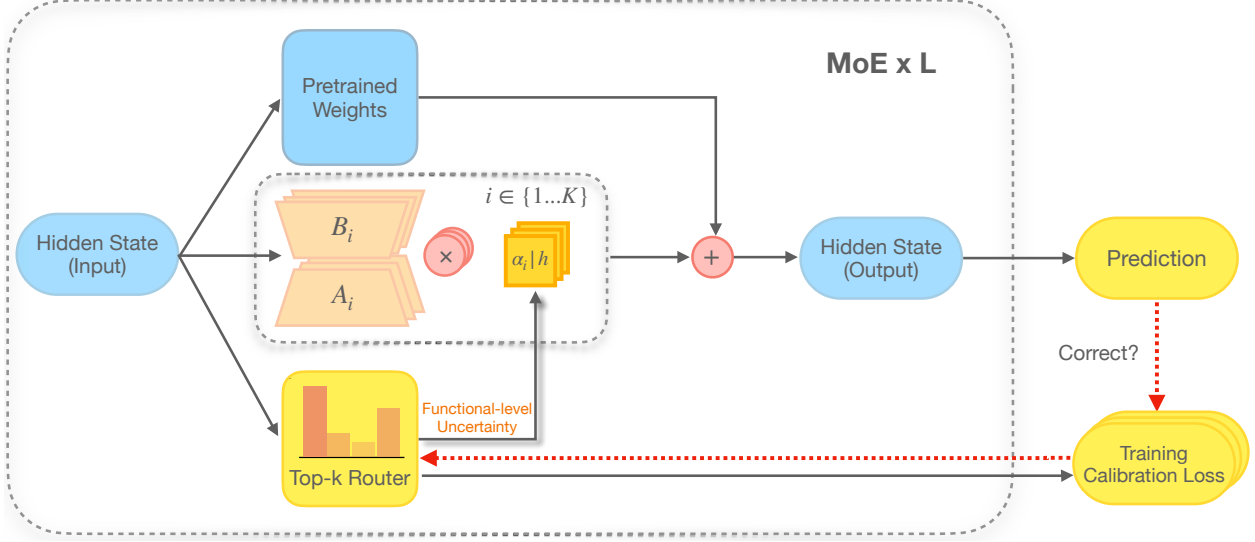


Figure 2: MoE architecture to capture functional-level uncertainty. LoRA experts (B_i, A_i) capture diverse functional bases, while the top- k router assigns mixture weights based on the input hidden state. The calibration loss aligns functional-level uncertainty with prediction correctness, encouraging confident expert selection for correct predictions and higher uncertainty for incorrect ones.

where each $g_{k^\ell}^\ell$ denotes a particular variant (e.g., LoRA-adapted) of the ℓ -th block and

$$g_{k^\ell}^\ell(\mathbf{h}^\ell) = \mathbf{h}^\ell + E_{k^\ell}^\ell(f_{trans}^\ell(\mathbf{h}^\ell)), \quad (7)$$

here f_{trans}^ℓ represents the necessary non-fine-tuned operations within a transformer block (i.e. layer norm, attention calculation, etc.) and as defined in Eq. 4, $E_{k^\ell}^\ell$ denotes the parameterized adaptation associated with the k^ℓ -th expert in the ℓ -th layer.

However, this naive decomposition is intractable in practice, as it requires keeping track of K^L mixture weights α_{k^1, \dots, k^L} . This is an exponential growth in the number of parameters with respect to both the number of layers L and the number of submodules per layer K , which makes the direct approach computationally infeasible for realistic network sizes.

Hierarchical Decomposition. To address the combinatorial explosion of mixture weights, we instead propose a hierarchical decomposition. Here, the mixture at each layer is formed independently, and the output of each layer is a weighted sum over its submodules, with the weights themselves being layer-specific:

$$f(\mathbf{x}) = \sum_{k^L=1}^K \alpha_{k^L}^L g_{k^L}^L \left(\dots \left(\sum_{k^l=1}^K \alpha_{k^l}^l g_{k^l}^l \left(\dots \sum_{k^1=1}^K \alpha_{k^1}^1 g_{k^1}^1(\mathbf{x}) \right) \right) \right). \quad (8)$$

Instead of needing K^L mixture weights, this hierarchical structure only requires $K \cdot L$ weights $\alpha_{k^\ell}^\ell$, one for each submodule in each layer. This dramatically reduces the parameters required and makes the decomposition tractable, while still enabling a rich set of compositional functions.

Dynamic, Input-Dependent Routing. To further enhance expressivity and efficiency, we allow the mixture weights to depend dynamically on the input at each layer. Specifically, we set the mixture weights to be a sparse routing function R^ℓ of the hidden state \mathbf{h}^ℓ at each layer, where $\alpha_{k^\ell}^\ell = \alpha_{k^\ell}^\ell(\mathbf{h}^\ell) = R_{k^\ell}^\ell(f_{trans}^\ell(\mathbf{h}^\ell))$.

Substituting this definition into the hierarchical mixture, the overall function $f(\mathbf{x})$ becomes:

$$f(\mathbf{x}) = \sum_{k^L=1}^K R_{k^L}^L(f_{trans}^L(\mathbf{h}^L)) g_{k^L}^L \left(\dots \left(\sum_{k^1=1}^K R_{k^1}^1(f_{trans}^1(\mathbf{h}^1)) g_{k^1}^1(\mathbf{x}) \right) \right). \quad (9)$$

This recursive formulation shows that at each layer, the submodules are weighted according to the input-dependent routing function, which adapts based on the current hidden state.

For a layer-wise perspective, the computation at each layer ℓ can be explicitly written as:

$$\mathbf{h}^{\ell+1} = \sum_{k^\ell=1}^K R_{k^\ell}^\ell(f_{trans}^\ell(\mathbf{h}^\ell)) g_{k^\ell}^\ell(\mathbf{h}^\ell). \quad (10)$$

Here, R^ℓ selects the most relevant submodules for a given input, allowing the network to adaptively compose its computation path at each layer in a sparse fashion.

3.2 Quantifying FLU with MixLoRA

In the previous section, we have established a parsimonious representation of the functional space. In this section, we choose a simple function to encode the functional level uncertainty and provide the intuition as follows. We first note that given a fixed MoE model architecture, the larger weight a mixture component has, the more certain we are about that component.

The model uncertainty of the MixLoRA architecture is quantified by considering perturbations $\Delta f(\mathbf{x})$ to the model $f(\mathbf{x})$. Following the discussion and notation in Sec. 3.1, we can show that these perturbations are instantiated in the space of the mixture weights α (as defined in Eq. 8 and 9):

Fact 3.1 (Model Perturbation Structure). *Under regularity assumptions on the residual connection architecture, perturbations $\Delta f(x)$ to the model $f(x)$ approximately decompose as:*

$$\Delta f(x) \approx \sum_{\ell=1}^L \sum_{k^\ell=1}^K \Delta \alpha_{k^\ell}^\ell(\mathbf{h}^\ell) \cdot g_{k^\ell}^\ell(\mathbf{h}^\ell).$$

In high-dimensional settings, the basis functions are approximately orthogonal. Thus, the perturbation $\Delta f(x)$ is entirely represented by the set $\{\Delta \alpha_{k^\ell}^\ell(\mathbf{h}^\ell)\}_{k^\ell=1, \dots, K}^{\ell=1, \dots, L}$. Therefore, the functional-level uncertainty (FLU) can be generally modeled as a linear function over the mixture weights:

$$\text{FLU}(x) = U \left(\{\alpha_{k^\ell}^\ell(\mathbf{h}^\ell)\}_{k^\ell=1, \dots, K}^{\ell=1, \dots, L} \right),$$

where $U(\cdot)$ denotes a linear aggregation function. Details of derivation is presented in Appendix A.1.

In practice, as illustrated in Figure 2, the top- k router at each layer produces a sparse probability vector $\alpha^\ell = (\alpha_1^\ell, \dots, \alpha_K^\ell)$, dynamically mixing the basis functions captured by the LoRA experts given the current hidden state. The values of the top- K routing weights that contribute to the final output hidden state serve as a direct quantification of the model’s uncertainty at functional-level. We follow the routing mechanisms used in MoE layers (see Eq. (3) and (4)), employing top-2 gate routers for the mixture. At each layer ℓ , we compute the raw router probabilities and retrain the largest two:

$$\tilde{R}^\ell(\mathbf{h}^\ell) = \text{Keep-Top-2}(\text{Softmax}(\mathbf{W}_r^\ell \cdot \mathbf{h}^\ell)). \quad (11)$$

Given an input prompt x of length s , we aggregate the router weights over the selected experts and across all layers to estimate the FLU:

$$\text{FLU}(x) = \frac{1}{L} \sum_{\ell=1}^L \sum_{i=1}^2 \tilde{R}_i^\ell(\mathbf{h}^\ell). \quad (12)$$

This formulation provides an efficient approach to quantify functional-level uncertainty in LoRA MoE architectures.

3.3 Calibration Loss

The FLU model provides a principled way to calibrate the mixture parameters against predictive accuracy, enabling better alignment between output distributions and true model confidence. Specifically, for MoE top- k routers, we design the following calibration loss for training:

$$\mathcal{L}_{\text{cal}} = (\mathbb{1}\{\text{MixLoRA}(x) = y^*\} - \text{FLU}(x))^2. \quad (13)$$

The first term is an indicator function that equals 1 if the model prediction matches the ground truth y^* for prompt x , and 0 otherwise, corresponding to a one-hot definition of ground truth confidence.

This calibration loss directly encourages the functional-level uncertainty (FLU) to reflect the true correctness of the model’s predictions. As shown in Figure 2, when the mixture model predicts correctly, the loss pushes FLU toward 1 (high confidence); when incorrect, toward 0 (low confidence). In other words, when optimized over the data distribution, the calibration loss pushes FLU to represent the probability of prediction correctness. We formally state this property as follows and present the proof in Appendix A.1:

Proposition 3.2 (Truthfulness of Calibration Loss). *Let the calibration risk be defined as the expectation of the calibration loss over the data distribution:*

$$\tilde{\mathcal{L}}_{\text{cal}} = \mathbb{E}_{(x, y^*) \sim \mathcal{D}} (\mathbb{1}\{\text{MixLoRA}(x) = y^*\} - \text{FLU}(x))^2.$$

If this calibration risk is optimized over the data distribution \mathcal{D} , then the optimal solution is $\text{FLU}(x) = \mathbb{P}(\text{MixLoRA}(x) = y^(x))$; that is, the optimally trained FLU corresponds to the probability that the model’s prediction is correct.*

3.4 Fine-tuning with the Total Loss

Our proposed calibration loss \mathcal{L}_{cal} improves predictive reliability by adaptively balancing expert exploitation and exploration according to functional-level uncertainty. As shown in Figure 2, \mathcal{L}_{cal} aligns uncertainty with predictive correctness, increasing the router probability of the selected expert for correct predictions (exploitation) and decreasing it for incorrect ones (exploration).

Ideally, when the K LoRA experts collectively capture the relevant functional relationships in the data during fine-tuning via cross-entropy loss, \mathcal{L}_{cal} further guides the model to select appropriate mixtures of LoRA experts conditioned on the input \mathbf{x} . This targeted selection enables the model to match the data distribution more closely and provides more calibrated uncertainty estimates.

To ensure balanced expert utilization, we incorporate a load balancing loss \mathcal{L}_b as proposed by Li et al. [2024]. Our overall loss function is:

$$\mathcal{L} = \text{CE} + \gamma \cdot \mathcal{L}_b + \beta \cdot \mathcal{L}_{\text{cal}}, \quad (14)$$

where CE is the cross-entropy loss, and γ, β are hyperparameters for the auxiliary terms. Details of \mathcal{L}_b are provided in Appendix A.2.

4 Related Work

Mixture of LoRA Experts. Large Language Models (LLMs) have achieved impressive performance across diverse NLP tasks [Brown et al., 2020, Hoffmann et al., 2022, Touvron et al., 2023b,c], with instruction fine-tuning [Chung et al., 2022, Iyer et al., 2022, Zheng et al., 2024] further boosting their adaptability for conversational AI [Wu et al., 2023b, Achiam et al., 2023]. However, scaling LLMs increases the resource demands of full fine-tuning. Parameter-efficient fine-tuning (PEFT) methods [Mangrulkar et al., 2022]—such as LoRA [Hu et al., 2021b] and its variants [Kopiczko et al., 2023, Hyeon-Woo et al., 2021, Renduchintala et al., 2023, Zhang et al., 2023, Liu et al., 2024]—reduce adaptation costs by updating a subset of parameters.

Recent advances combine PEFT with the Mixture-of-Experts (MoE) framework [Jacobs et al., 1991, Wang et al., 2020], which sparsely activates expert subnetworks for greater model capacity and specialization. MoE-based LLMs leverage expert routing and parameter-efficient adaptations to target new domains or tasks efficiently. Notably, methods such as MoRAL [Yang et al., 2024b], LoRAMoE [Dou et al., 2024], PESC [Wu et al., 2024b], MoE-LoRA [Luo et al., 2024], and MixLoRA [Li et al., 2024] optimize domain-specific routing, mitigate forgetting, and enable scalable, high-throughput training and inference with mixtures of LoRA experts.

Uncertainty Quantification in LLMs. Established uncertainty quantification methods have been studied in conjunction with the LoRA structure for LLMs. Monte-Carlo dropout [Gal and Ghahramani, 2016] interprets dropout in neural networks as approximate Bayesian inference in deep Gaussian processes, allowing uncertainty estimates to be obtained from existing LoRA adapters without modifying them. Checkpoint ensemble [Chen et al., 2017] utilizes predictions from multiple LoRA checkpoints saved during a single fine-tuning process to calibrate uncertainty. Deep ensemble [Lakshminarayanan et al., 2017, Wang et al., 2023, Zhai et al., 2023] combines the predictions from multiple LoRA adapters for better uncertainty calibration. Laplace-LoRA [Yang et al., 2024a] applies Bayesian inference via Laplace approximation to the LoRA parameters after fine-tuning, resulting in improved calibration and uncertainty estimates.

Prompt-perturbation and resampling-based approaches have also been explored for uncertainty quantification in LLMs. These methods estimate uncertainty by measuring prediction variability under different prompt formulations or sampled input variants, without altering model parameters [Farquhar et al., 2024, Hou et al., 2023, Gao et al., 2024]. This line of work leverages the inherent sensitivity of LLMs to input perturbations as a means to assess model confidence, providing a complementary perspective to parameter-based methods. Ye et al. [2024] benchmark LLMs using conformal prediction, which quantifies uncertainty by constructing prediction sets with guaranteed coverage, where set size directly reflects model uncertainty.

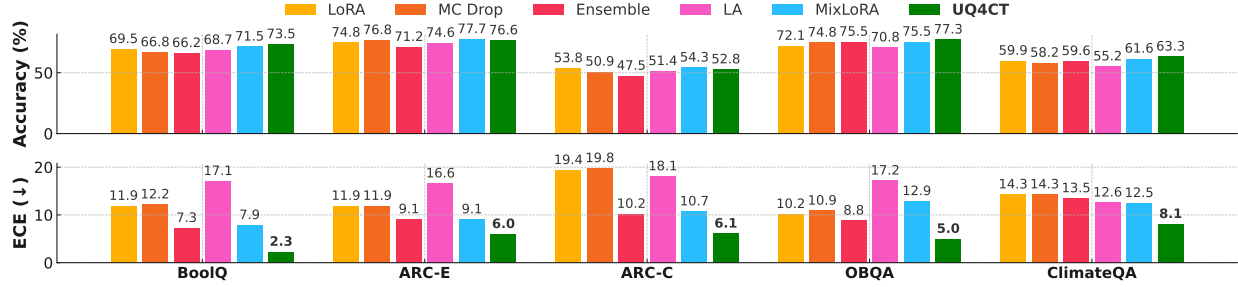


Figure 3: Performance comparison of different methods fine-tuned with LLaMA2-7B across four common sense reasoning tasks and a domain-specific task. UQ4CT shows substantial ECE improvements while maintaining high accuracy.

5 Experiments

Datasets. We evaluate on five multiple-choice QA benchmarks: OpenBookQA (OBQA) [Mihaylov et al., 2018], ARC-Easy (ARC-E) and ARC-Challenge (ARC-C) [Clark et al., 2018], BoolQ [Clark et al., 2019], and ClimateQA—a domain-specific climate science benchmark. To assess robustness under distribution shift, we ensemble the domain-specific MMLU subtasks [Hendrycks et al., 2020] into 4 benchmarks focusing on different professionalities: Computer Science (CS), Engineering (Eng), Law and Health. Details for the ensemble are provided in Appendix A.8. Models are fine-tuned on the public training split and evaluated on the test split for each benchmark.

Experiment Setup. We implement UQ4CT with PyTorch [Paszke et al., 2019], extending the MixLoRA repository in [Li et al., 2024]. We use the LLaMA-2-7B-hf [Touvron et al., 2023a] as our base model. In particular, we apply MixLoRA to query, key, value and output layers, together with the feed-forward networks in LLaMA-2-7B-hf (gate layer, down layer and up layer). Details are provided in Appendix A.6.

- **LoRA** [Hu et al., 2021a]. We use standard LoRA fine-tuning as lower performance bound.
- **Monte Carlo (MC) Dropout** [Gal and Ghahramani, 2016] keeps dropout on at both training and testing time. By performing multiple forward passes, MC dropout randomly shuts down a portion of model nodes, producing ensemble-like predictions. To combine LoRA fine-tuning with MC dropout, we apply dropout on the input of the LoRA adapter, following the implementation of Mangrulkar et al. [2022].
- **Deep Ensemble** [Lakshminarayanan et al., 2017] averages the predictions from each ensemble member which have been trained with varying random initialization. We combine deep ensemble with LoRA by fine-tuning 3 randomly initialized LoRAs together and ensembling their output as final predictions.
- **Laplace-LoRA (LA)** [Yang et al., 2024a] applies a post-hoc Laplace approximation on fine-tuned LoRA parameters for better uncertainty estimation.
- **MixLoRA** [Li et al., 2024] incorporates LoRAs via a router network to reduce computational overhead while expanding model capacity. We add this as a baseline to resemble plain LoRA MoE model performance.

Evaluation. We evaluate prediction accuracy on the validation set across all five tasks. For uncertainty calibration, we use the expected calibration error (ECE; Guo et al. [2017]; more details in A.7) to measure the alignment between predicted probabilities and actual outcomes.

To assess robustness under distribution shifts, we fine-tune models on the OBQA dataset and evaluate them following [Yang et al., 2024a]. We use ARC-C and ARC-E to represent smaller distribution shifts, as these datasets focus on general science reasoning similar to OBQA but are more challenging and diverse. For larger shifts, we utilize the four aforementioned domain-specific MMLU subtasks, which span a wide range of expertise from elementary to professional levels. This domain specificity represents a greater distribution shift from the general common sense focus of OBQA.

The in-distribution scenario tests model alignment on the target task, while the distribution shift scenario assesses generalizability to novel domains. Together, they provide a comprehensive evaluation for real-world applications, ensuring strong performance on the primary task and resilience to out-of-distribution inputs.

5.1 In-distribution Performance

As shown in Figure 3, UQ4CT achieves notable gains in uncertainty calibration across diverse tasks, while maintaining competitive accuracy (ACC) relative to baseline approaches. For instance, on BoolQ and ClimateQA tasks, UQ4CT

Table 1: Performance comparison of different methods fine-tuned on the OBQA dataset with LLaMA2-7B across two smaller distribution shift (DS) tasks and four larger distribution shift tasks. UQ4CT shows substantial ECE improvements while maintaining high accuracy.

Metrics	Methods	ID	Smaller DS		Larger DS			
		OBQA	ARC-C	ARC-E	CS	Eng	Law	Health
ACC \uparrow	LoRA	72.1 _{0.87}	58.6 _{1.93}	66.5 _{3.38}	35.5 _{2.35}	30.8 _{1.72}	34.9 _{1.41}	39.1 _{1.52}
	MC Drop	74.8 _{1.34}	58.7 _{2.07}	66.6 _{3.30}	36.0 _{1.69}	30.3 _{2.25}	35.1 _{0.86}	39.1 _{1.35}
	Ensemble	75.5 _{1.4}	57.7 _{0.78}	69.1 _{0.48}	36.7_{2.18}	30.3 _{1.13}	35.3 _{1.02}	39.9 _{1.89}
	LA	70.8 _{1.24}	58.7 _{0.58}	67.9 _{0.41}	33.7 _{1.22}	29.6 _{1.32}	35.4 _{0.75}	38.5 _{1.61}
	MixLoRA	75.5 _{2.91}	58.5 _{1.44}	69.2_{1.02}	35.2 _{2.92}	30.3 _{0.98}	35.9_{0.43}	40.6_{1.13}
	UQ4CT	77.3_{1.36}	58.8_{1.06}	65.8 _{1.31}	36.2 _{1.24}	34.1_{2.31}	35.8 _{1.01}	40.0 _{1.24}
ECE \downarrow	LoRA	10.2 _{1.07}	16.7 _{2.28}	13.3 _{2.48}	29.7 _{2.69}	32.3 _{1.85}	29.2 _{3.08}	31.0 _{2.13}
	MC Drop	10.9 _{0.24}	16.7 _{2.20}	13.2 _{2.21}	23.2 _{2.32}	31.6 _{1.64}	28.0 _{2.93}	25.9 _{2.27}
	Ensemble	8.83 _{2.35}	15.1 _{1.09}	11.1 _{0.99}	22.4 _{1.32}	28.5 _{2.13}	29.0 _{1.37}	24.5 _{0.39}
	LA	17.2 _{1.2}	16.2 _{0.5}	24.4 _{0.42}	28.6 _{2.61}	30.5 _{1.43}	29.5 _{1.83}	30.7 _{1.2}
	MixLoRA	12.9 _{1.99}	19.0 _{1.88}	14.5 _{2.57}	26.4 _{3.25}	33.7 _{1.87}	30.3 _{2.27}	28.3 _{1.07}
	UQ4CT	5.0_{1.15}	8.9_{3.46}	6.5_{1.85}	19.6_{2.90}	23.1_{1.17}	25.9_{3.43}	21.9_{3.49}

Table 2: Performance of UQ4CT with varying β values on the OBQA dataset. Prediction accuracy and uncertainty calibration improve with increasing β , highlighting the effectiveness of \mathcal{L}_{cal} .

β	0	0.2	0.5	0.8	1	1.2	1.5	1.8	2
ACC \uparrow	75.5 _{2.91}	76.0 _{0.6}	75.9 _{0.31}	76.6 _{0.4}	77.3 _{1.36}	77.9_{0.6}	77.2 _{0.91}	76.7 _{0.82}	76.6 _{0.92}
ECE \downarrow	12.9 _{1.99}	7.47 _{0.78}	7.82 _{0.93}	5.94 _{1.16}	5.0_{1.15}	6.49 _{2.65}	9.19 _{0.86}	8.11 _{1.43}	6.65 _{1.85}

attains accuracy rates of 73.5% and 63.3%, demonstrating that improved uncertainty quantification does not come at the expense of predictive performance.

The most significant improvements are seen in reduced Expected Calibration Error (ECE). UQ4CT consistently lowers ECE by over 25% on average across benchmarks, and unlike other approaches, it continues to perform well even on challenging datasets such as ARC-C, achieving an ECE of 6.1.

To further validate our method, we include results from fine-tuning both LLaMA-2-7B (main text) and Mistral-7B (Appendix A.3). Across both models, UQ4CT delivers substantial and consistent improvements in uncertainty calibration. These results underscore the practical value of UQ4CT, particularly in scenarios where reliable uncertainty estimates are crucial, such as safety-critical applications. A key advantage of UQ4CT is that it incorporates uncertainty calibration directly during fine-tuning, incurring minimal computational overhead compared to other uncertainty quantification (UQ) methods, which often require costly repetitive sampling or post-hoc adjustments.

5.2 Performance Under Distribution Shift

Due to the sparse nature of the fine-tuning data, real world deployment of LLMs often requires the model to be robust to out-of-distribution knowledge [Ouyang et al., 2022, Touvron et al., 2023d,a]. Therefore, we evaluate the performance of UQ4CT along with other baseline models fine-tuned on the OBQA dataset under smaller and larger distribution shift scenarios.

Table 1 presents the distribution shift evaluations. UQ4CT achieves substantial ECE improvements while maintaining high accuracy across both smaller and larger distribution shifts. For smaller shifts, UQ4CT’s ECE remains comparable to the in-distribution scenario. Under larger shifts, UQ4CT attains the lowest ECE among all baselines and delivers competitive accuracy on all domain-specific tasks. These results demonstrate that aligning uncertainty at the functional level with predictive correctness improves generalizability and mitigates overconfidence in fine-tuned models.

5.3 Ablation Studies

We conduct ablation studies to investigate the effectiveness of our designed calibration loss, \mathcal{L}_{cal} . We first perform a sensitivity test, in which we explore the impact of \mathcal{L}_{cal} on the overall performance. Then we evaluate the incremental weighting performance of the calibration term in Appendix A.4, which investigates the effectiveness of \mathcal{L}_{cal} at the early stage of fine-tuning. We also conduct an ablation study on the impact of active LoRA experts in Appendix A.5.

Sensitivity Test on Calibration Term. To further understand the effectiveness of the calibration loss, we perform a sensitivity test of the coefficient β in Equation 14. This evaluates how our proposed calibration of parameter mixtures affect the overall model prediction and uncertainty quantification capabilities. We evaluate β values ranging from 0 to 2, where $\beta = 0$ resembles the original MixLoRA method.

Results in Table 2 demonstrate the effectiveness of the calibration loss. When $\beta = 0$, the model is optimized without calibration on parameter mixtures, resulting in high ECE value. Even with small $\beta = 0.2$ or $\beta = 0.5$, the ECE scores drastically improved compared to no calibration setting. Finally, when $\beta = 1$, the calibration term effectively optimizes the conditional parameter mixtures to generate outputs that fit data distribution well, resulting in lower ECE scores and higher accuracies.

6 Discussion & Conclusion

In this work, we propose Functional-Level Uncertainty Quantification for Calibrated Fine-Tuning (UQ4CT), which addresses the overconfidence issues commonly encountered during fine-tuning of large language models. We present a functional perspective on quantifying uncertainty in LLMs and utilize it for uncertainty-calibrated fine-tuning. By incorporating functional-level uncertainty quantification with a mixture-of-experts framework, our proposed uncertainty-calibrated training loss effectively addresses the challenge of overconfidence in fine-tuned LLMs by significantly improving uncertainty calibration while maintaining high accuracy. Our evaluations demonstrate that UQ4CT reduces the Expected Calibration Error by more than 25% without compromising accuracy across a variety of downstream tasks, including common-sense and domain-specific reasoning, under in-distribution and out-of-distribution scenarios.

The limitation of UQ4CT lies in its dependency on predictive correctness. For general language modeling tasks such as chat completion, there lacks a clear metric on response correctness. This limits the application of UQ4CT as naively token matching is a poor indicator of semantic correctness due to the ambiguous nature of language. For future work, we are exploring ways to adapt UQ4CT to open-ended problems that lack a definitive optimization objective.

Acknowledgement

This work was supported in part by U. S. Army Research Office under Army-ECASE award W911NF-07-R-0003-03, the U.S. Department Of Energy, Office of Science, IARPA HAYSTAC Program, and NSF Grants #2205093, #2146343, #2134274, CDC-RFA-FT-23-0069, DARPA AIE FoundSci and DARPA YFA.

References

- Yupeng Chang, Xu Wang, Jindong Wang, Yuan Wu, Linyi Yang, Kaijie Zhu, Hao Chen, Xiaoyuan Yi, Cunxiang Wang, Yidong Wang, et al. A survey on evaluation of large language models. *ACM Transactions on Intelligent Systems and Technology*, 15(3):1–45, 2024.
- Yuxin Xiao, Paul Pu Liang, Umang Bhatt, Willie Neiswanger, Ruslan Salakhutdinov, and Louis-Philippe Morency. Uncertainty quantification with pre-trained language models: A large-scale empirical analysis. In *EMNLP*, 2022.
- Guande He, Jianfei Chen, and Jun Zhu. Preserving pre-trained features helps calibrate fine-tuned language models. In *ICLR*, 2023.
- Katherine Tian, Eric Mitchell, Allan Zhou, Archit Sharma, Rafael Rafailov, Huaxiu Yao, Chelsea Finn, and Christopher D Manning. Just ask for calibration: Strategies for eliciting calibrated confidence scores from language models fine-tuned with human feedback. *arXiv preprint arXiv:2305.14975*, 2023.
- OpenAI. GPT-4 technical report, 2023.
- Karan Singhal, Shekoofeh Azizi, Tao Tu, S. Sara Mahdavi, Jason Wei, Hyung Won Chung, Nathan Scales, Ajay Tanwani, Heather Cole-Lewis, Stephen Pfohl, Perry Payne, Martin Seneviratne, Paul Gamble, Chris Kelly, Nathaneal Scharli, Aakanksha Chowdhery, Philip Mansfield, Blaise Agüera y Arcas, Dale Webster, Greg S. Corrado, Yossi Matias, Katherine Chou, Juraj Gottweis, Nenad Tomasev, Yun Liu, Alvin Rajkomar, Joelle Barral, Christopher Semturs, Alan Karthikesalingam, and Vivek Natarajan. Large Language Models Encode Clinical Knowledge. *arXiv*, 2022.
- Shijie Wu, Ozan Irsoy, Steven Lu, Vadim Dabravolski, Mark Dredze, Sebastian Gehrmann, Prabhanjan Kambadur, David Rosenberg, and Gideon Mann. BloombergGPT: A Large Language Model for Finance, May 2023a.
- Andrew Kyle Lampinen, Stephanie C. Y. Chan, Ishita Dasgupta, Andrew J. Nam, and Jane X. Wang. Passive learning of active causal strategies in agents and language models, May 2023.
- Shuang Li, Xavier Puig, Chris Paxton, Yilun Du, Clinton Wang, Linxi Fan, Tao Chen, De-An Huang, Ekin Akyürek, Anima Anandkumar, et al. Pre-trained language models for interactive decision-making. *Advances in Neural Information Processing Systems*, 35:31199–31212, 2022.
- Bairu Hou, Yujian Liu, Kaizhi Qian, Jacob Andreas, Shiyu Chang, and Yang Zhang. Decomposing uncertainty for large language models through input clarification ensembling, 2023.
- Xiang Gao, Jiaxin Zhang, Lalla Mouatadid, and Kamalika Das. Spuq: Perturbation-based uncertainty quantification for large language models. *arXiv preprint arXiv:2403.02509*, 2024.
- Sebastian Farquhar, Jannik Kossen, Lorenz Kuhn, and Yarin Gal. Detecting hallucinations in large language models using semantic entropy. *Nature*, 630(8017):625–630, 2024.
- Edward J Hu, Yelong Shen, Phillip Wallis, Zeyuan Allen-Zhu, Yuanzhi Li, Shean Wang, Lu Wang, and Weizhu Chen. Lora: Low-rank adaptation of large language models. *arXiv preprint arXiv:2106.09685*, 2021a.
- Yarin Gal and Zoubin Ghahramani. Dropout as a bayesian approximation: Representing model uncertainty in deep learning. In *international conference on machine learning*, pages 1050–1059. PMLR, 2016.
- Hugh Chen, Scott Lundberg, and Su-In Lee. Checkpoint ensembles: Ensemble methods from a single training process. *arXiv preprint arXiv:1710.03282*, 2017.
- Balaji Lakshminarayanan, Alexander Pritzel, and Charles Blundell. Simple and scalable predictive uncertainty estimation using deep ensembles. *Advances in neural information processing systems*, 30, 2017.
- Xi Wang, Laurence Aitchison, and Maja Rudolph. Lora ensembles for large language model fine-tuning. *arXiv preprint arXiv:2310.00035*, 2023.
- Yuanzhao Zhai, Han Zhang, Yu Lei, Yue Yu, Kele Xu, Dawei Feng, Bo Ding, and Huaimin Wang. Uncertainty-penalized reinforcement learning from human feedback with diverse reward lora ensembles. *arXiv preprint arXiv:2401.00243*, 2023.
- Adam X. Yang, Maxime Robeyns, Xi Wang, and Laurence Aitchison. Bayesian low-rank adaptation for large language models, 2024a.
- Dengchun Li, Yingzi Ma, Naizheng Wang, Zhiyuan Cheng, Lei Duan, Jie Zuo, Cal Yang, and Mingjie Tang. Mixlora: Enhancing large language models fine-tuning with lora based mixture of experts. *arXiv preprint arXiv:2404.15159*, 2024.
- Hugo Touvron, Louis Martin, Kevin Stone, Peter Albert, Amjad Almahairi, Yasmine Babaei, Nikolay Bashlykov, Soumya Batra, Prajjwal Bhargava, Shruti Bhosale, et al. Llama 2: Open foundation and fine-tuned chat models. *arXiv preprint arXiv:2307.09288*, 2023a.

- Xun Wu, Shaohan Huang, and Furu Wei. Mixture of lora experts. *arXiv preprint arXiv:2404.13628*, 2024a.
- Dmitry Lepikhin, HyoukJoong Lee, Yuanzhong Xu, Dehao Chen, Orhan Firat, Yanping Huang, Maxim Krikun, Noam Shazeer, and Zhifeng Chen. Gshard: Scaling giant models with conditional computation and automatic sharding. In *ICLR*, 2020.
- Tom B. Brown, Benjamin Mann, Nick Ryder, Melanie Subbiah, Jared Kaplan, Prafulla Dhariwal, Arvind Neelakantan, Pranav Shyam, Girish Sastry, Amanda Askell, Sandhini Agarwal, Ariel Herbert-Voss, Gretchen Krueger, T. J. Henighan, Rewon Child, Aditya Ramesh, Daniel M. Ziegler, Jeff Wu, Clemens Winter, Christopher Hesse, Mark Chen, Eric Sigler, Mateusz Litwin, Scott Gray, Benjamin Chess, Jack Clark, Christopher Berner, Sam McCandlish, Alec Radford, Ilya Sutskever, and Dario Amodei. Language models are few-shot learners. *ArXiv*, abs/2005.14165, 2020. URL <https://api.semanticscholar.org/CorpusID:218971783>.
- Jordan Hoffmann, Sebastian Borgeaud, Arthur Mensch, Elena Buchatskaya, Trevor Cai, Eliza Rutherford, Diego de Las Casas, Lisa Anne Hendricks, Johannes Welbl, Aidan Clark, Tom Hennigan, Eric Noland, Katie Millican, George van den Driessche, Bogdan Damoc, Aurelia Guy, Simon Osindero, Karen Simonyan, Erich Elsen, Jack W. Rae, Oriol Vinyals, and L. Sifre. Training compute-optimal large language models. *ArXiv*, abs/2203.15556, 2022. URL <https://api.semanticscholar.org/CorpusID:247778764>.
- Hugo Touvron, Thibaut Lavril, Gautier Izacard, Xavier Martinet, Marie-Anne Lachaux, Timothée Lacroix, Baptiste Rozière, Naman Goyal, Eric Hambro, Faisal Azhar, Aurelien Rodriguez, Armand Joulin, Edouard Grave, and Guillaume Lample. Llama: Open and efficient foundation language models. *ArXiv*, abs/2302.13971, 2023b. URL <https://api.semanticscholar.org/CorpusID:257219404>.
- Hugo Touvron, Louis Martin, Kevin R. Stone, Peter Albert, Amjad Almahairi, Yasmine Babaei, Nikolay Bashlykov, Soumya Batra, Prajjwal Bhargava, Shruti Bhosale, Daniel M. Bikel, Lukas Blecher, Cristian Cantón Ferrer, Moya Chen, Guillem Cucurull, David Esiobu, Jude Fernandes, Jeremy Fu, Wenyin Fu, Brian Fuller, Cynthia Gao, Vedanuj Goswami, Naman Goyal, Anthony S. Hartshorn, Saghar Hosseini, Rui Hou, Hakan Inan, Marcin Kardas, Viktor Kerkez, Madian Khabsa, Isabel M. Kloumann, A. V. Korenev, Punit Singh Koura, Marie-Anne Lachaux, Thibaut Lavril, Jenya Lee, Diana Liskovich, Yinghai Lu, Yuning Mao, Xavier Martinet, Todor Mihaylov, Pushkar Mishra, Igor Molybog, Yixin Nie, Andrew Poulton, Jeremy Reizenstein, Rashi Rungta, Kalyan Saladi, Alan Schelten, Ruan Silva, Eric Michael Smith, R. Subramanian, Xia Tan, Binh Tang, Ross Taylor, Adina Williams, Jian Xiang Kuan, Puxin Xu, Zhengxu Yan, Iliyan Zarov, Yuchen Zhang, Angela Fan, Melanie Kambadur, Sharan Narang, Aurelien Rodriguez, Robert Stojnic, Sergey Edunov, and Thomas Scialom. Llama 2: Open foundation and fine-tuned chat models. *ArXiv*, abs/2307.09288, 2023c. URL <https://api.semanticscholar.org/CorpusID:259950998>.
- Hyung Won Chung, Le Hou, S. Longpre, Barret Zoph, Yi Tay, William Fedus, Eric Li, Xuezhi Wang, Mostafa Dehghani, Siddhartha Brahma, Albert Webson, Shixiang Shane Gu, Zhuyun Dai, Mirac Suzgun, Xinyun Chen, Aakanksha Chowdhery, Dasha Valter, Sharan Narang, Gaurav Mishra, Adams Wei Yu, Vincent Zhao, Yanping Huang, Andrew M. Dai, Hongkun Yu, Slav Petrov, Ed Huai hsin Chi, Jeff Dean, Jacob Devlin, Adam Roberts, Denny Zhou, Quoc V. Le, and Jason Wei. Scaling instruction-finetuned language models. *ArXiv*, abs/2210.11416, 2022. URL <https://api.semanticscholar.org/CorpusID:253018554>.
- Srinivas Iyer, Xi Victoria Lin, Ramakanth Pasunuru, Todor Mihaylov, Daniel Simig, Ping Yu, Kurt Shuster, Tianlu Wang, Qing Liu, Punit Singh Koura, Xian Li, Brian O’Horo, Gabriel Pereyra, Jeff Wang, Christopher Dewan, Asli Celikyilmaz, Luke Zettlemoyer, and Veselin Stoyanov. Opt-1ml: Scaling language model instruction meta learning through the lens of generalization. *ArXiv*, abs/2212.12017, 2022. URL <https://api.semanticscholar.org/CorpusID:255096269>.
- Lianmin Zheng, Wei-Lin Chiang, Ying Sheng, Siyuan Zhuang, Zhanghao Wu, Yonghao Zhuang, Zi Lin, Zhuohan Li, Dacheng Li, Eric Xing, et al. Judging llm-as-a-judge with mt-bench and chatbot arena. *NeurIPS*, 36, 2024.
- Tianyu Wu, Shizhu He, Jingping Liu, Siqi Sun, Kang Liu, Qing-Long Han, and Yang Tang. A brief overview of chatgpt: The history, status quo and potential future development. *IEEE/CAA Journal of Automatica Sinica*, 10(5):1122–1136, 2023b.
- Josh Achiam, Steven Adler, Sandhini Agarwal, Lama Ahmad, Ilge Akkaya, Florencia Leoni Aleman, Diogo Almeida, Janko Altschmidt, Sam Altman, Shyamal Anadkat, et al. Gpt-4 technical report. *arXiv preprint arXiv: 2303.08774*, 2023.
- Sourab Mangrulkar, Sylvain Gugger, Lysandre Debut, Younes Belkada, and Sayak Paul. Peft: State-of-the-art parameter-efficient fine-tuning methods. <https://github.com/huggingface/peft>, 2022.
- J. Edward Hu, Yelong Shen, Phillip Wallis, Zeyuan Allen-Zhu, Yuanzhi Li, Shean Wang, and Weizhu Chen. Lora: Low-rank adaptation of large language models. *ArXiv*, abs/2106.09685, 2021b. URL <https://api.semanticscholar.org/CorpusID:235458009>.

- Dawid Jan Kopiczko, Tijmen Blankevoort, and Yuki Markus Asano. Vera: Vector-based random matrix adaptation. *arXiv preprint arXiv: 2310.11454*, 2023.
- Nam Hyeon-Woo, Moon Ye-Bin, and Tae-Hyun Oh. Fedpara: Low-rank hadamard product for communication-efficient federated learning. *arXiv preprint arXiv: 2108.06098*, 2021.
- Adithya Renduchintala, Tugrul Konuk, and Oleksii Kuchaiev. Tied-lora: Enhancing parameter efficiency of lora with weight tying. *arXiv preprint arXiv: 2311.09578*, 2023.
- Qingru Zhang, Minshuo Chen, Alexander Bukharin, Pengcheng He, Yu Cheng, Weizhu Chen, and Tuo Zhao. Adaptive budget allocation for parameter-efficient fine-tuning. In *ICLR*, 2023.
- Shih-Yang Liu, Chien-Yi Wang, Hongxu Yin, Pavlo Molchanov, Yu-Chiang Frank Wang, Kwang-Ting Cheng, and Min-Hung Chen. Dora: Weight-decomposed low-rank adaptation. *arXiv preprint arXiv: 2402.09353*, 2024.
- Robert A. Jacobs, Michael I. Jordan, Steven J. Nowlan, and Geoffrey E. Hinton. Adaptive mixtures of local experts. *Neural Computation*, 1991.
- Xin Wang, Fisher Yu, Lisa Dunlap, Yi-An Ma, Ruth Wang, Azalia Mirhoseini, Trevor Darrell, and Joseph E Gonzalez. Deep mixture of experts via shallow embedding. In *Uncertainty in artificial intelligence*, pages 552–562. PMLR, 2020.
- Shu Yang, Muhammad Asif Ali, Cheng-Long Wang, Lijie Hu, and Di Wang. Moral: Moe augmented lora for llms’ lifelong learning. *arXiv preprint arXiv: 2402.11260*, 2024b.
- Shihan Dou, Enyu Zhou, Yan Liu, Songyang Gao, Jun Zhao, Wei Shen, Yuhao Zhou, Zhiheng Xi, Xiao Wang, Xiaoran Fan, Shiliang Pu, Jiang Zhu, Rui Zheng, Tao Gui, Qi Zhang, and Xuanjing Huang. Loramoe: Alleviate world knowledge forgetting in large language models via moe-style plugin. *arXiv*, 2024.
- Haoyuan Wu, Haisheng Zheng, and Bei Yu. Parameter-efficient sparsity crafting from dense to mixture-of-experts for instruction tuning on general tasks. *arXiv preprint arXiv: 2401.02731*, 2024b.
- Tongxu Luo, Jiahe Lei, Fangyu Lei, Weihao Liu, Shizhu He, Jun Zhao, and Kang Liu. Moelora: Contrastive learning guided mixture of experts on parameter-efficient fine-tuning for large language models. *arXiv preprint arXiv: 2402.12851*, 2024.
- Fanghua Ye, Yang MingMing, Jianhui Pang, Longyue Wang, Derek F Wong, Yilmaz Emine, Shuming Shi, and Zhaopeng Tu. Benchmarking llms via uncertainty quantification. *arXiv preprint arXiv:2401.12794*, 2024.
- Todor Mihaylov, Peter Clark, Tushar Khot, and Ashish Sabharwal. Can a suit of armor conduct electricity? a new dataset for open book question answering. In *EMNLP*, 2018.
- Peter Clark, Isaac Cowhey, Oren Etzioni, Tushar Khot, Ashish Sabharwal, Carissa Schoenick, and Oyvind Tafjord. Think you have solved question answering? try arc, the ai2 reasoning challenge. *arXiv preprint arXiv:1803.05457*, 2018.
- Christopher Clark, Kenton Lee, Ming-Wei Chang, Tom Kwiatkowski, Michael Collins, and Kristina Toutanova. Boolq: Exploring the surprising difficulty of natural yes/no questions. *arXiv preprint arXiv:1905.10044*, 2019.
- Dan Hendrycks, Collin Burns, Steven Basart, Andy Zou, Mantas Mazeika, Dawn Song, and Jacob Steinhardt. Measuring massive multitask language understanding. *arXiv preprint arXiv:2009.03300*, 2020.
- Adam Paszke, Sam Gross, Francisco Massa, Adam Lerer, James Bradbury, Gregory Chanan, Trevor Killeen, Zeming Lin, Natalia Gimelshein, Luca Antiga, et al. Pytorch: An imperative style, high-performance deep learning library. *Advances in neural information processing systems*, 32, 2019.
- Chuan Guo, Geoff Pleiss, Yu Sun, and Kilian Q Weinberger. On calibration of modern neural networks. In *International conference on machine learning*, pages 1321–1330. PMLR, 2017.
- Long Ouyang, Jeffrey Wu, Xu Jiang, Diogo Almeida, Carroll Wainwright, Pamela Mishkin, Chong Zhang, Sandhini Agarwal, Katarina Slama, Alex Ray, et al. Training language models to follow instructions with human feedback. *Advances in Neural Information Processing Systems*, 35:27730–27744, 2022.
- Hugo Touvron, Thibaut Lavril, Gautier Izacard, Xavier Martinet, Marie-Anne Lachaux, Timothée Lacroix, Baptiste Rozière, Naman Goyal, Eric Hambro, Faisal Azhar, et al. Llama: Open and efficient foundation language models. *arXiv preprint arXiv:2302.13971*, 2023d.
- Albert Q Jiang, Alexandre Sablayrolles, Arthur Mensch, Chris Bamford, Devendra Singh Chaplot, Diego de las Casas, Florian Bressand, Gianna Lengyel, Guillaume Lample, Lucile Saulnier, et al. Mistral 7b. *arXiv preprint arXiv: 2310.06825*, 2023.

A Appendix

A.1 Theoretical Derivation of the Method

In this section, we provide complete theoretical statements and proofs that are used in Sec. 3 to derive our method.

Fact A.1 (Model Perturbation Structure, Restatement of Fact 3.1). *Assume that in the residual connection architecture in each layer: $g_{k^\ell}^\ell(\mathbf{h}^\ell) = \mathbf{h}^\ell + E_{k^\ell}^\ell(f_{trans}^\ell(\mathbf{h}^\ell))$, the Lipschitzness of the residual term $E_{k^\ell}^\ell(f_{trans}^\ell(\mathbf{h}^\ell))$ is much smaller as compared to that of \mathbf{h}^ℓ itself: $\|E_{k^\ell}^\ell(f_{trans}^\ell(\hat{\mathbf{h}}^\ell)) - E_{k^\ell}^\ell(f_{trans}^\ell(\mathbf{h}^\ell))\| = o(\|\hat{\mathbf{h}}^\ell - \mathbf{h}^\ell\|)$. Under this regularity assumption, perturbations $\Delta f(x)$ to the model $f(x)$ approximately decomposes as:*

$$\Delta f(x) \approx \sum_{\ell=1}^L \sum_{k^\ell=1}^K \Delta \alpha_{k^\ell}^\ell(\mathbf{h}^\ell) \cdot g_{k^\ell}^\ell(\mathbf{h}^\ell).$$

Proof of Fact 3.1 and A.1. In each layer, we can decompose the perturbation to the output as follows:

$$\Delta \mathbf{h}^{\ell+1} = \sum_{k^\ell=1}^K [\Delta \alpha_{k^\ell}^\ell(\mathbf{h}^\ell) \cdot g_{k^\ell}^\ell(\mathbf{h}^\ell) + \alpha_{k^\ell}^\ell(\mathbf{h}^\ell) \cdot \Delta g_{k^\ell}^\ell(\mathbf{h}^\ell)], \quad \forall \ell = 1, \dots, L,$$

where the input $\mathbf{h}^1 = x$ and the output $f(x) = \mathbf{h}^{L+1}$.

Due to the residual connection architecture and our assumption on the regularity of the residual term, we have:

$$\Delta g_{k^\ell}^\ell(\mathbf{h}^\ell) = \Delta \mathbf{h}^\ell + \Delta E_{k^\ell}^\ell(f_{trans}^\ell(\mathbf{h}^\ell)) = \Delta \mathbf{h}^\ell + o(\Delta \mathbf{h}^\ell).$$

Hence,

$$\Delta \mathbf{h}^{\ell+1} \approx \sum_{k^\ell=1}^K (\Delta \alpha_{k^\ell}^\ell(\mathbf{h}^\ell) \cdot g_{k^\ell}^\ell(\mathbf{h}^\ell) + \alpha_{k^\ell}^\ell(\mathbf{h}^\ell) \cdot \Delta \mathbf{h}^\ell) = \sum_{k^\ell=1}^K \Delta \alpha_{k^\ell}^\ell(\mathbf{h}^\ell) \cdot g_{k^\ell}^\ell(\mathbf{h}^\ell) + \Delta \mathbf{h}^\ell.$$

Expanding this recursion, the output perturbation can be approximated as:

$$\Delta f(x) = \Delta \mathbf{h}^{L+1} \approx \sum_{\ell=1}^L \sum_{k^\ell=1}^K \Delta \alpha_{k^\ell}^\ell(\mathbf{h}^\ell) \cdot g_{k^\ell}^\ell(\mathbf{h}^\ell).$$

□

Proposition A.2 (Calibration Loss, Restatement of Proposition 3.2). *Let the calibration risk be defined as the expectation of the calibration loss over the data distribution:*

$$\bar{\mathcal{L}}_{\text{cal}} = \mathbb{E}_{(x, y^*) \sim \mathcal{D}} (\mathbb{1}\{\text{MixLoRA}(x) = y^*\} - \text{FLU}(x))^2.$$

If this calibration risk is optimized over the data distribution \mathcal{D} , then the optimal solution is $\text{FLU}(x) = \mathbb{P}(\text{MixLoRA}(x) = y^(x))$; that is, the optimally trained FLU corresponds to the probability that the model's prediction is correct.*

Proof of Proposition 3.2 and A.2. Expanding the calibration risk, we have:

$$\begin{aligned} \bar{\mathcal{L}}_{\text{cal}} &= \mathbb{E}_{(x, y^*) \sim \mathcal{D}} (\mathbb{1}\{\text{MixLoRA}(x) = y^*\} - \text{FLU}(x))^2 \\ &= \mathbb{E}_{(x, y^*) \sim \mathcal{D}} [\mathbb{1}\{\text{MixLoRA}(x) = y^*\}]^2 \\ &\quad - 2 \mathbb{E}_x \mathbb{E}_{y^*|x} [\mathbb{1}\{\text{MixLoRA}(x) = y^*\} \cdot \text{FLU}(x)] + \mathbb{E}_x [\text{FLU}(x)^2] \\ &= C + \mathbb{E}_x [\text{FLU}(x)^2 - 2 \mathbb{P}(\text{MixLoRA}(x) = y^*(x)) \cdot \text{FLU}(x)], \end{aligned}$$

where C is a constant independent of $\text{FLU}(x)$. Thus, the calibration risk is minimized when $\text{FLU}(x) = \mathbb{P}(\text{MixLoRA}(x) = y^*(x))$. □

Table 3: Performance comparison of UQ4CT with and without incremental weighting. Incremental weighting has worse ECE performance while maintains similar accuracy.

Metrics	Methods	BoolQ	ARC-E	ARC-C	OBQA	ClimateQA
ACC \uparrow	UQ4CT	73.5 _{0.52}	76.6 _{1.30}	52.8 _{1.77}	77.3 _{1.36}	63.3 _{1.74}
	UQ4CT_Incremental	72.0 _{0.19}	75.4 _{0.81}	54.6 _{0.95}	77.6 _{0.43}	60.2 _{3.17}
ECE \downarrow	UQ4CT	2.30_{0.82}	6.00_{0.2}	6.11_{1.11}	5.01_{1.15}	8.10_{0.52}
	UQ4CT_Incremental	4.0 _{0.16}	9.8 _{1.51}	13.8 _{2.08}	10.3 _{1.73}	12.2 _{0.88}

Table 4: Performance comparison of different methods fine-tuned with Mistral-7B across 4 common sense reasoning tasks and a domain-specific task. UQ4CT shows significant ECE improvements while maintaining high accuracy.

Metrics	Methods	BoolQ	ARC-E	ARC-C	OBQA	ClimateQA
ACC \uparrow	LoRA	70.3 _{0.62}	84.8 _{0.47}	70.2 _{0.84}	82.8 _{0.62}	72.5 _{1.6}
	MC Drop	69.6 _{1.07}	84.6 _{0.91}	69.6 _{0.76}	82.6 _{0.71}	72.5 _{1.6}
	Ensemble	71.8 _{1.29}	84.2 _{0.66}	71.0 _{1.41}	82.5 _{0.6}	72.9 _{2.88}
	LA	70.7 _{1.82}	82.4 _{2.05}	68.5 _{3.31}	82.5 _{0.77}	71.6 _{1.56}
	MixLoRA	73.1 _{0.38}	85.5 _{1.27}	71.2 _{1.75}	83.3 _{1.14}	72.0 _{1.69}
	UQ4CT	73.60_{0.28}	85.90_{0.82}	74.40_{0.82}	83.71_{0.22}	73.21_{0.29}
ECE \downarrow	LoRA	10.17 _{0.24}	9.46 _{1.62}	18.42 _{1.91}	13.3 _{0.25}	13.72 _{2.62}
	MC Drop	10.62 _{0.51}	8.91 _{1.35}	18.38 _{1.66}	13.3 _{0.31}	13.72 _{2.61}
	Ensemble	8.72 _{1.13}	8.72 _{1.49}	17.0 _{0.97}	9.14 _{2.82}	12.86 _{1.78}
	LA	5.33 _{2.16}	20.3 _{5.7}	21.27 _{4.15}	6.41_{3.22}	14.64 _{2.21}
	MixLoRA	8.81 _{1.03}	8.16 _{0.99}	15.51 _{3.86}	10.53 _{1.73}	14.05 _{3.09}
	UQ4CT	3.070_{0.83}	5.70_{0.69}	7.040_{0.58}	<u>7.92_{1.14}</u>	11.41_{1.14}

A.2 Load Balancing Loss

We follow the load balancing loss in [Li et al., 2024]. Given N experts indexed by $i = 1$ to N and a batch B with T tokens, the auxiliary loss is computed as:

$$\mathcal{L}_{aux} = a \cdot N \cdot \sum_{i=1}^N \mathcal{F}_i \cdot \mathcal{P}_i, \quad (15)$$

where

$$\mathcal{F}_i = \frac{1}{T} \sum_{x \in B} \mathbb{1}\{\argmax_k \mathcal{R}(x)_k = i\}, \mathcal{P}_i = \frac{1}{T} \sum_{x \in B} \mathcal{R}(x)_i. \quad (16)$$

Here, $\mathcal{R}(\cdot)$ is the top-k router, \mathcal{F}_i is the fraction of tokens dispatched to expert i and \mathcal{P}_i is the fraction of the router probability allocated for expert i . The final loss is multiplied by the expert count N to keep the loss constant as the number of experts varies, and the constant term a is set to 10^{-2} as a multiplicative coefficient, which is large enough to ensure load balancing while remaining small enough not to overwhelm the primary objective.

A.3 Experimental Results with Mistral-7B

In this section, we present the results using Mistral-7B [Jiang et al., 2023], a different decoder-based LLM backbone. Table 4 shows the results of fine-tuning Mistral-7B on 4 common-sense reasoning tasks and one domain-specific climate question-answering task.

For each of the tasks, UQ4CT effectively calibrates the parameter mixtures, leading to the best ECE performance in 4 out of 5 tasks. This indicates the robustness of UQ4CT across different LLMs.

A.4 Incremental Weighting on Calibration Term

Due to the random initialization of LoRA experts, the predictions during early fine-tuning stage are likely to be incorrect as the model has little knowledge on the functional relationships regarding the data. Thus, it is intuitive to incrementally increase the weight parameter β over the calibration term \mathcal{L}_{cal} in the training loss for the LoRA experts to learn before calibration. We conduct this study by incrementally increase β from 0 to 1 within 50 gradient steps during the early stage of fine-tuning:

$$\beta = \min \left\{ 1, \frac{\text{current_grad_step}}{50} \right\}. \quad (17)$$

Table 5: Performance comparison of UQ4CT with varying number of experts on OBQA dataset. Top-2 expert selection strategy grants best accuracy and calibration.

Top-K	ACC \uparrow	ECE \downarrow
Top-1	74.8 _{0.62}	7.69 _{1.96}
Top-2	77.3_{1.36}	5.0_{1.15}
Top-3	75.2 _{0.8}	5.8 _{0.81}
Top-4	75.8 _{0.53}	7.67 _{0.46}
Top-5	75.3 _{0.5}	6.29 _{0.61}

We choose 50 gradient steps from our observation that training loss generally stabilizes after 50 gradient steps, indicating the LoRA experts have learned some functional relationships from data.

As shown in Table 3, the incremental loss has significantly worse ECE performance across all tasks. This demonstrates the advantage of uncertainty calibration even in the early stage. In the beginning, the lack of functional relationships on the training data in LoRA experts lead to high functional-level uncertainty. Thus, UQ4CT encourages exploration over all LoRA experts while UQ4CT_Incremental lacks it due to the small weighting in the beginning.

A.5 Deciding Number of Active Experts

One important aspect of the LoRA MoE architecture is how many experts to activate. Here, we investigate the performance impact of different number of active LoRA experts. We evaluate the model performance with 1 to 5 active experts with 8 in total.

As shown in Table 5, 2 active experts give the optimal performance in terms of accuracy and ECE scores. One expert alone cannot capture complicated functional relationships, while more than 2 experts could potentially introduce redundant functional bases to the model, which deviates the output distribution more from data distribution, thus worsening predictive and calibration performance. Additionally, more active experts lead to a more flattened distribution across experts, which hardens the alignment of parameter mixtures during fine-tuning.

A.6 Training Details

We train our model with total of 8 LoRA experts, and select 2 experts with the highest probability. For each expert, we use $rank = 16$ and $alpha = 32$. We use batch size of 16 to train our model. For climate task, we set the learning rate to $5e - 4$ and dropout rate to 0.1 to incorporate the small dataset size. For other tasks, we use $2e - 4$ as our learning rate with dropout 0.05. We use AdamW as our optimizer and a cutoff length of 512 for prompts during training. Our model is trained on A100 GPU, with 20GB GPU memory consumption per task. Training time is from 25 to 50 minutes depending on the task.

The experimental setup for single LoRA based models is similar with LoRA ranks set to 80 to accommodate the MoE model size. For the ensemble baseline, we use an ensemble size of 8 with $rank = 16$. For Laplace-LoRA, we follow the Laplace hyperparameters in this Github Repository.

A.7 Expected Calibration Error

Expected calibration error (ECE) is a commonly used metric to asses uncertainty quantification performance. ECE measures the alignment between prediction accuracy and model confidence through regrouping the predicted probabilities into m bins. This method then computes the weighted average of the difference between average accuracy and confidence in each bin:

$$ECE = \sum_{m=1}^M \frac{|B_m|}{N} |\text{acc}(B_m) - \text{conf}(B_m)|, \quad (18)$$

where $|B_m|$ is the number of evaluated datapoints in bin m , acc and conf is calculated as following:

$$\text{acc}(B_m) = \frac{1}{|B_m|} \sum_{i \in B_m} \mathbf{1}(\hat{y}_i = y_i), \quad (19)$$

$$\text{conf}(B_m) = \frac{1}{|B_m|} \sum_{i \in B_m} P(\hat{y}_i). \quad (20)$$

In this paper, we use an ECE bin size of 15, following the experiment setup in Laplace-LoRA [Yang et al., 2024a].

A.8 MMLU Distribution Shift Dataset Composition

- **Computer Science (CS):**
 - College Computer Science
 - Computer Security
 - High School Computer Science
 - Machine Learning
- **Engineering (Eng):**
 - Electrical Engineering
- **Law:**
 - International Law
 - Jurisprudence
 - Professional Law
- **Health:**
 - Anatomy
 - Clinical Knowledge
 - College Medicine
 - Human Aging
 - Nutrition
 - Professional Medicine
 - Virology

A.9 Prompt Perturbation Comparison

Here, we compare our method with SPUQ [Gao et al., 2024], which perturbs the prompt, aggregates predictions and confidences to measure uncertainty. We test SPUQ and UQ4CT with LLama2-7b as the base model. As shown in Table 6, SPUQ’s large ECE values suggest that simply aggregating predictions from perturbed prompts does not adequately calibrate model confidence, highlighting the limitations of prompt perturbation as an uncertainty quantification strategy for LLMs, especially for smaller models.

Table 6: Performance comparison of UQ4CT and SPUQ across five tasks. UQ4CT achieves higher accuracy and substantially lower ECE than SPUQ.

Metrics	Methods	BoolQ	ARC-E	ARC-C	OBQA	ClimateQA
ACC \uparrow	SPUQ	62.20	75.14	45.99	59.00	60.64
	UQ4CT	73.5 _{0.52}	76.6 _{1.30}	52.8 _{1.77}	77.3 _{1.36}	63.3 _{1.74}
ECE \downarrow	SPUQ	30.47	13.13	24.74	20.00	19.98
	UQ4CT	2.3 _{0.82}	6.0 _{0.2}	6.1 _{1.11}	5.0 _{1.15}	8.1 _{0.52}